Wu *et al. Chin. J. Mech. Eng.* (2018) 31:94
https://doi.org/10.1186/s10033-018-0290-x

Chinese Journal of Mechanical Engineering

ORIGINAL ARTICLE

Open Access

# A New Grasping Mode Based on a Sucked-type Underactuated Hand

Pei-Chen Wu*, Nan Lin, Ting Lei, Qian Cheng, Jin-Ze Wu and Xiao-Ping Chen

**Abstract**

Robot hands have been developing during the last few decades. There are many mechanical structures and analytical methods for different hands. But many tough problems still limit robot hands to apply in homelike environment. The ability of grasping objects covering a large range of sizes and various shapes is fundamental for a home service robot to serve people better. In this paper, a new grasping mode based on a novel sucked-type underactuated (STU) hand is proposed. By combining the flexibility of soft material and the effect of suction cups, the STU hand can grasp objects with a wide range of sizes, shapes and materials. Moreover, the new grasping mode is suitable for some situations where the force closure is failure. In this paper, we deduce the effective range of sizes of objects which our hand using the new grasping mode can grasp. Thanks to the new grasping mode, the ratio of grasping size between the biggest object and the smallest is beyond 40, which makes it possible for our robot hand to grasp diverse objects in our daily life. For example, the STU hand can grasp a soccer (220 mm diameter, 420 g) and a fountain pen (9 mm diameter, 9 g). What's more, we use the rigid body equilibrium conditions to analysis the force condition. Experiment evaluates the high load capacity, stability of the new grasping mode and displays the versatility of the STU hand. The STU hand has a wide range of applications especially in unstructured environment.

**Keywords:** Grasping mode, Underactuated hand, Sucked-type, Stability of new mode, Grasping diverse objects

## 1 Introduction

Grasping is a significant function for robots especially for home service robots. In an unstructured environment such as homelike environment, diverse grasping seems to be essential to manipulate objects of different shapes and sizes [1]. Obviously, human hand has been the most dexterous hand up to now in this field. So many researches imitate structure and grasping mode of human hand. Moreover, there are other structures designed differently.

The dexterous hands, whose number of actuators is no less than the number of degrees of freedom, have been presented over 30 years [2]. Many different approaches have been proposed through the decades, such as UTAH/MIT hand [3], Robonaut [4], Gifu hand II [5], DLR-HIT-Hand [6]. And recently, there is a DLR Hand-Arm system [7] which has 52 actuators and 19 degrees of freedom. These hands can be controlled accurately so that they achieve dexterity in some degree. But they are expensive to manufacture because of the numerous actuators and sensors and they are computationally complex [8, 9].

Another approach is to let the number of actuators less than the number of degrees of freedom [10, 11]. These hands can adapt the shape of object by utilizing flexible materials. Traditionally, the underactuated hands consist of phalanxes and joints [12–14]. The former is rigid and the latter always has flexibility [2]. In recent years, soft robot grippers actuated by pneumatic actuator have been widely studied [15–18]. This kind of fingers will bend by inflating the pneumatic actuators like pneumatic networks or PneuFlex. Soft robots are considered to be safer, more adaptable and compliant than the rigid robots [19]. And its capability to perform effective grasping has been proved [1]. While grasping, the underactuated hand can adapt itself to the contour of objects because of compliance of the materials used. So it is easy to control these hands. And they are lightweight on account of a smaller number of actuators. Even so, these hands still remain many deficiencies, one of which is that they can not grasp

*Correspondence: iewupeichen@163.com
School of Computer Science and Technology, University of Science and Technology of China, Hefei 230000, China

large object like soccer. There are also other novel gripper, for example, some grippers make use of granular jamming transition to pick objects up [20, 21].

When grasping, except for the structure, choosing a suitable grasping mode is also important. And analyzing the grasping mode can guide the design of mechanical structure of hand. Many researches have been presented on grasping taxonomies. Some of them attempt to categorize grasping modes by studying grasps of human hand while others study the physical and mechanical properties of the hand, the object, and the contact [22]. The physiological approach has many different classifications because the points they focused on are diverse. For instance, Cutkosky and Wright [23] focus on machine environment, Lyons [24] bases his classification on precision, and Iberall [25] wants to simplify the taxonomy by using virtual fingers [22]. All of these taxonomies are influenced by power grasping and precision grasping which were introduced by Napier [26]. For the mechanical and physical approach, the well-known force closure [27] and form closure [28] were presented. Bud Mishra and Naomi Silver consider the force closure and form closure are equivalent [22].

Although there are many structures and analysis modes, there is still a long way for robotic hand to achieve the performance of human hand. Not to mention some grasping tasks are even difficult for most human, for example grasping a soccer with only one hand. And the force closure analysis is also a failure according to the study of Nguyen [29]. To some extent, it is poor performance of robotic hands and lack of grasping mode that prohibit the application in home.

We aim at designing a hand that can achieve diverse grasping in homelike environment. In prior work, we proposed an underactuated hand whose size is same as human hand combining the passive compliance of soft materials and the suction force of suction cups to realize this goal. In this paper, we present a new grasping mode for our hand to grasp large object like soccer and small object like fountain pen. We demonstrate that the equilibrium conditions for grasping large object are similar to the ones for pinching small object in Section 3. And then, we evaluate the stability of the new grasping mode. To our best knowledge, it is the first time for the anthropomorphic hand to reach such a large range of grasping size.

For the rest of the paper, design of the STU hand and definition of the new grasping mode are applied first. Then we deduce the effective range of sizes of objects grasped by the new grasping mode. In the same part, we analyze the force condition when grasping object. In addition, experiment evaluates the high load capacity, stability of the new grasping mode and displays the versatility of the STU hand. And the final section summarizes the study.

## 2 Design of the STU Hand and Definition of a New Grasping Mode

### 2.1 Design of the STU Hand

In our prior work, we designed a gripper combing underactuated technology with suction cups. As shown in Figure 1, the gripper has tendon-driven system, 3D-printing base, and two symmetrical flexible fingers on which the suction cups are embedded. Silica gel skin is used to cover the finger for improving friction force on contact surface. The Table 1 displays the intrinsic parameters of the gripper, which are shown in Figure 1.

During grasping procedure, steel wire shortens as a result of spooler motor rotating. Then the PVC board generates elastic deformation, the finger is bent and the gripper closes. Thanks to the flexibility of the PVC board, the gripper can be well compliant with the contour of object and suction cups will produce negative pressure to help grasp once it contacts the object. And we can configure different stiffness of each joint by changing the thickness of PVC board. According to experiment, if the finger-root moves prior than fingertip without touching object by configuring suitable stiffness, the hand performs better. Furthermore, the curvature of the finger can not be negative (the finger opens outward) avoiding damaging the finger.

The vacuum system shown in Figure 2 also plays an important role in the gripper. Mini vacuum pump which can produce maximal −80 kPa pressure connect with suction cups through solenoid valve. Computer controls the working state of gas circuit through the Microprogrammed Control Unit (MCU). If the solenoid valve is opened, the suction cup is connected with mini vacuum

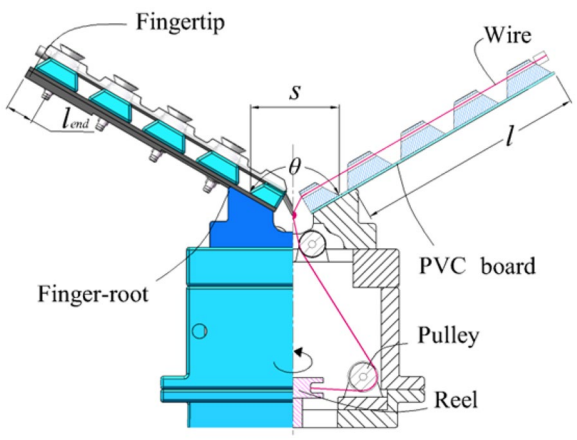


**Figure 1** CAD model and schematic diagram of the STU hand

**Table 1 Parameters and their description**

| Parameter name | Description |
|---|---|
| $s$ | The distance between two root of fingers |
| $\theta$ | The initial angle between two fingers |
| $l$ | The finger length |
| $l_{end}$ | The distance between fingertip and the nearest suction cup's center |

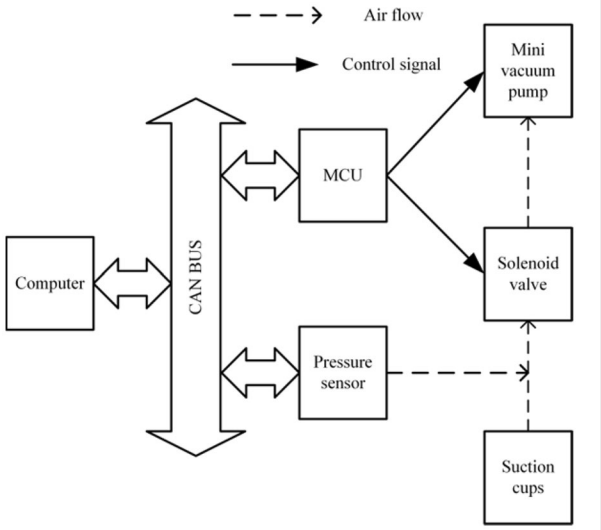


**Figure 2** Control framework of vacuum system

pump. Whereas, if the solenoid is closed, its pressure is equal to the air pressure. And the MCU can capture the pressure data from the pressure sensor obeying the Pascal's principle.

### 2.2 Definition of a New Grasping Mode

#### *2.2.1 Definition*

The gripper grasping the object, if the gripper has a component force in the grasping force that ejects the object from the gripper, if and only if the reverse force provided by the particular mechanical structures of the gripper (e.g., vacuum suction, electromagnetic force) can counteract with this component force, the object is grasped by the gripper steadily. The mode which mainly uses characteristics of reverse force to grasp object is defined as half-enveloping mode.

According to characteristics of the gripper structure, our gripper can implement two types of half-enveloping grasping. For convenience, we simplify the target object into a cylinder (Generally, objects have external cylinder).

#### *2.2.2 Big Object Half-Enveloping (BOHE)*

As is often the case in the life, the size of objects we want to grasp is large than our palms' size. This mode, however, can easily solve the problem as shown in Figure 3(a). As the finger's movement is resisted by the object, the root of fingers can't bend, that fingertips will bend to attach the object. In this case, the contact surface length is less than half of the circumference of the object. If the grasping force works alone, the object will be pushed away from the gripper.

#### *2.2.3 Small Object Half-Enveloping (SOHE)*

The another extreme situation is that the objects are too small to hold in the hand. Usually, we human tend to pinch it with two fingers, while our STU hand grasps them with the SOHE grasping mode as shown in Figure 3(b). As the root of fingers takes precedence over the fingertip to move, only the root of fingers bend and the fingertips hardly bend. At this point, the contact surface length is less than half of the circumference of the object, and the target object will be pushed away without the suction force (towards palm).

The force diagram of grasping the large object is shown in Figure 4. The arrows represent the positive pressure and suction generated by fingers. Bow-tied shaped sectors are the friction cones. At this moment, the resultant force of the positive pressure of the gripper on the object causes the object away from the gripper, while the suction provided by the vacuum pump counteract this resultant force. According to previous study on two-fingers gripper by Jean Ponce, as shown in Figure 4, this situation doesn't meet the condition of the force-closure, but it is in line with half-enveloping grasping condition. Our gripper can grasp object steadily in this case. In other words, some objects which don't achieve force closure can be grasped by adapting the Half-Enveloping mode. Grasping small objects is similar to the large ones.

## 3 Analysis of Object Size and Grasping Force

### 3.1 Object Size Analysis

In the following $N$, $M$, $P$, $A$ and $O$ indicate the mark points of the fingers and the object respectively. As shown in Figure 5(a), the radius of the object is $R$, the object center is $O$, the origin of the base is $N$. the root of the finger and the base are linked at $M$, the bend part and

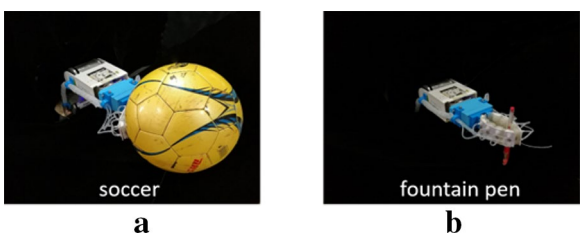


**Figure 3** Grasp soccer and fountain pan

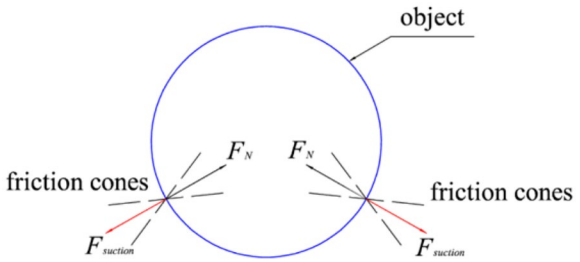


**Figure 4** Displaying the force condition of grasping object with two fingers

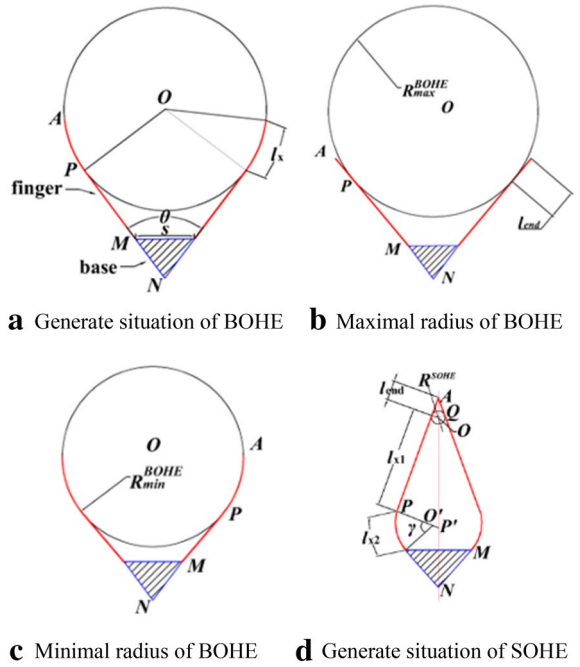


**a** Generate situation of BOHE **b** Maximal radius of BOHE

**c** Minimal radius of BOHE **d** Generate situation of SOHE

**Figure 5** Grasping schematic diagram of BOHE and SOHE

the unbend part of the finger are tangent at $P$, and the fingertip is $A$.

#### 3.1.1 Size Analysis of BOHE

When objects has relatively large radios, they will resist the fingers. The fingertip will bend when grasping. And as a result of the flexibility of the material, the bend part will be compliant with the surface of the object. The length of finger sticking on the object is $l_x$, so $\overline{PM} = l - l_x$. In the $\Delta ONP$, yielding

$$R = \overline{OP} = \left( \frac{s}{2\sin\frac{\theta}{2}} + l - l_x \right) \tan\frac{\theta}{2}. \tag{1}$$

When the object and the finger are tangent at the suction cup which locates the end of the finger, the finger can directly suck up the object without bending, as shown in Figure 5(b) with $l_x = l_{end}$. Then the maximal object size of the BOHE mode can be expressed as

$$R^{BOHE}_{\max} = \left( \frac{s}{2\sin\frac{\theta}{2}} + l - l_{end} \right) \tan\frac{\theta}{2}. \tag{2}$$

There is another situation that when an object is grasped, its diameter happens to be the distance between the two fingertips, then the object size is considered as the minimal object size. As the Figure 5(c) shows, in the case $l_x$ has a maximum value as $R \times \theta/2$, and the minimal size can be obtained as

$$R^{BOHE}_{\min} = \frac{s + 2l\sin\frac{\theta}{2}}{2\cos\frac{\theta}{2} + \theta\sin\frac{\theta}{2}}. \tag{3}$$

#### 3.1.2 Size Analysis of SOHE

When grasping small objects, as the Figure 5(d) shows, only the root of finger will bend because of the configuration of stiffness on different joints. And the radius of curvature of the arc which results of the bend is $\gamma$. Joints near to the fingertip will be unbent and two fingertips will contact with each other with an included angle measuring $\beta$. Then there are only suction cups which locate at the fingertip stick on the object. The finger and the object are tangent at $Q$ ($Q$ is the circle center of the fingertip suction cup) with $\overline{QA} = l_{end}$.

All points and parameters of the finger are depicted in Figure 5(d). Obviously, the whole length of the finger $l$ equals to $l_{end} + l_{x1} + l_{x2}$. It can be expressed by the Geometric relationship that $\beta/2 = \gamma - \theta/2$. The extended line of radius $PQ'$ and the symmetry axis of the gripper intersect at $P'$. So we can obtain that

$$\overline{PP'} = \frac{\frac{s}{2} - r\cos\frac{\theta}{2}}{\cos\frac{\beta}{2}} + r = (l - l_{x2})\tan\frac{\beta}{2}, \tag{4}$$

where $r = l_{x2}/\gamma$. Then we can deduce the minimum object size of the SOHE

$$R^{SOHE} = l_{end}\tan\frac{\beta}{2}. \tag{5}$$

### 3.2 Grasping Force Analysis

In this part, the bold face represents vector. And we assume finger point contact with Coulomb friction. Many assumptions are made in this part to improve simulation performance and enable higher fidelity results.

### 3.2.1 Grasping Force Analysis of BOHE

In order to evaluate gripper's ability to grasp column in half-enveloping grasping mode, the evaluation criteria are the maximum of the tension $\boldsymbol{F}_1$ (including the object's gravity) and the lateral disturbing force $\boldsymbol{F}_2$ that the gripper can resist when grasping. The bounds of $\boldsymbol{F}_1$ and $\boldsymbol{F}_2$ can be derived in the case of force balance.

Firstly, we carry out mechanical analysis of gripper when it grasps big objects. Figure 6 shows more details of static analysis model. It is assumed that the finger and object are tangent at the last suction cup since suction cups are small and uniformly attached to the surface of fingers. Each finger has $n$ sets of suction cups contacting with object and each set has two suction cups which can provide negative pressure $P$ on the area of $S$. When the STU hand holds object, the positive pressure provided by finger is $\boldsymbol{F}_{Ni}$. Suction cups can offer the suction force $\boldsymbol{F}_p$, the static friction force $\boldsymbol{F}_f$, the tension $\boldsymbol{F}_1$ and the lateral disturbing force $\boldsymbol{F}_2$. Additionally, we assume that max stiction of all suction cup is reached at the same time. Other parameters of the gripper were displayed before.

By observing Figure 6(a), we can obtain that the length of flank of base is

$$l_s = \frac{s}{2\sin\frac{\theta}{2}}. \tag{6}$$

Then the radius of object can be expressed as:

$$R = (l - l_x + l_s)\tan\frac{\theta}{2}. \tag{7}$$

The distance between two suction cups is

$$\Delta x = \frac{l_x}{n-1}. \tag{8}$$

The central angle of $\Delta x$ can be obtained as follows:

$$\Delta\alpha = \frac{l_x}{(n-1)R} \tag{9}$$

Next we will discuss rigid equilibrium which is shown in Figure 6(a). For resultant moment, the direction of all force points to the center of the circle except static friction force. The suction cup on the left side is located at the point $A_i$ and another one on the right side is at $A_i'$. The static friction force, suction force produced by vacuum pump and positive pressure produced by fingers from both sides reach a balance in the direction $y$ and overlay in the $z$ direction. So we have:

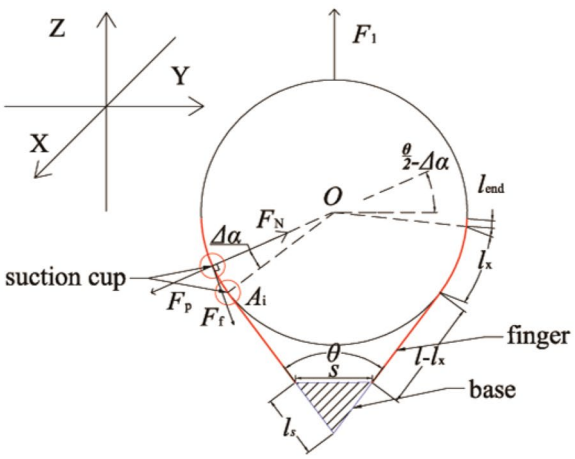


**a** Schematic diagram of tension

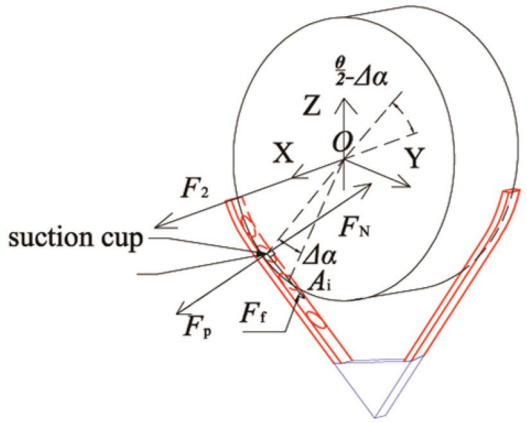


**b** Schematic diagram of lateral disturbing force

**Figure 6** Grasping schematic diagram of BOHE

$$\begin{cases} \sum \boldsymbol{\mathcal{L}} = \sum_{i=0}^{n-1}(\boldsymbol{\mathcal{F}}_{fi} \times \boldsymbol{\mathcal{A}}_i\boldsymbol{\mathcal{O}}) + \sum_{i=0}^{n-1}(\boldsymbol{\mathcal{F}}'_{fi} \times \boldsymbol{\mathcal{A}}'_i\boldsymbol{\mathcal{O}}) = \boldsymbol{0}, \\ F_P = 2PS, \\ F_{fi\max} = \mu(F_{Ni} + 2PS), \\ F_{fi\max_z} = F_{fi\max}\cos\left(\frac{\theta}{2} - i\Delta\alpha\right), \\ F_{Ni_z} = F_{Ni}\sin\left(\frac{\theta}{2} - i\Delta\alpha\right), \\ F_{P_z} = F_P\sin\left(\frac{\theta}{2} - i\Delta\alpha\right), \\ F_1 + 2\sum_{i=0}^{n-1}(F_{Ni_z} - F_{P_z}) \le 2\sum_{i=0}^{n-1}F_{fi\max_z}. \end{cases} \tag{10}$$

Combining Eqs. (6)–(10) and simplifying result in

$$F_{1\max} = 2\left[\sum_{i=0}^{n-1}\mu(F_{Ni} + 2PS)\cos\left(\frac{\theta}{2} - \frac{il_x\cot\frac{\theta}{2}}{(n-1)\left(l - l_x + \frac{s}{2\sin\frac{\theta}{2}}\right)}\right) - \sum_{i=0}^{n-1}(F_{Ni} - 2PS)\sin\left(\frac{\theta}{2} - \frac{il_x\cot\frac{\theta}{2}}{(n-1)\left(l - l_x + \frac{s}{2\sin\frac{\theta}{2}}\right)}\right)\right]. \tag{11}$$

For lateral disturbing force, mechanical analysis is familiar to static friction force. The pressures from the two fingers balance in the $y$ direction but overlay in the $z$ direction as well as suction force. At the same time, static friction forces from the two fingers balance in the $y$ direction but overlay in the $xz$ plane. So we have:

$$\begin{cases} \sum \boldsymbol{\mathcal{L}} = \sum_{i=0}^{n-1}(\boldsymbol{\mathcal{F}}_{fi} \times \boldsymbol{\mathcal{A}}_i\boldsymbol{\mathcal{O}}) + \sum_{i=0}^{n-1}(\boldsymbol{\mathcal{F}}'_{fi} \times \boldsymbol{\mathcal{A}}'_i\boldsymbol{\mathcal{O}}) = \boldsymbol{0}, \\ F_P = 2PS, \\ F_{fi\max} = \mu(F_{Ni} + 2PS), \\ F_{fi\,\max_{xz}} = F_{fi\max}\cos\left(\frac{\theta}{2} - i\Delta\alpha\right), \\ F_{Ni_z} = F_{Ni}\sin\left(\frac{\theta}{2} - i\Delta\alpha\right), \\ F_{P_z} = F_P\sin\left(\frac{\theta}{2} - i\Delta\alpha\right), \\ F_2^2 + \sum_{i=0}^{n-1}(2F_{Ni_z} - 2F_{P_z})^2 \le \sum_{i=0}^{n-1}(2F_{fi\,\max_{xz}})^2. \end{cases} \tag{12}$$

Combining Eqs. (6)–(9) and (12), then simplifying result in

$$F_{2\max} = 2\left\{\left[\sum_{i=0}^{n-1}\mu(2PS + F_{Ni})\cos\left(\frac{\theta}{2} - \frac{il_x\cot\frac{\theta}{2}}{(n-1)(l - l_x + \frac{s}{2\sin\frac{\theta}{2}})}\right)\right]^2 - \left[\sum_{i=0}^{n-1}(F_{Ni} - 2PS)\sin\left(\frac{\theta}{2} - \frac{il_x\cot\frac{\theta}{2}}{(n-1)(l - l_x + \frac{s}{2\sin\frac{\theta}{2}})}\right)\right]^2\right\}^{\frac{1}{2}} \tag{13}$$

### 3.2.2 Grasping Force Analysis of SOHE

When it comes to the size of small object, the model can be simplified further which is shown in Figure 7. We assume there are two suction cups attached to objects, which can provide the positive pressure $\boldsymbol{F}_N$. The angle between the two fingertips is

$$\alpha = 2\arctan\frac{r}{l_{x1} + l_{end}}, \tag{14}$$

where $r = 2l_{x2}/(\alpha + \beta)$. In this situation, the analysis method of the tension on object shown in Figure 7(a) is the same as tension of BOHE. The force condition is:

$$\begin{cases} \sum \boldsymbol{\mathcal{L}} = (\boldsymbol{\mathcal{F}}_f \times \boldsymbol{\mathcal{A}}\boldsymbol{\mathcal{O}}) + (\boldsymbol{\mathcal{F}}'_f \times \boldsymbol{\mathcal{A}}'\boldsymbol{\mathcal{O}}) = \boldsymbol{0}, \\ F_P = 2PS, \\ F_{f\max} = \mu(F_N + 2PS), \\ F_{f\,\max_z} = F_{f\max}\cos\frac{\alpha}{2}, \\ F_{N_z} = F_N\sin\frac{\alpha}{2}, \\ F_{P_z} = F_P\sin\frac{\alpha}{2}, \\ F_1 + 2F_{N_z} - 2F_{P_z} \le 2F_{f\,\max_z}. \end{cases} \tag{15}$$

Combining Eqs. (14), (15) and simplifying result in

$$F_{1\max} = 2\left[\mu(F_N + 2PS)\cos\left(\arctan\left(\frac{r}{l_{x1} + l_{end}}\right)\right) - (F_N - 2PS)\sin\left(\arctan\left(\frac{r}{l_{x1} + l_{end}}\right)\right)\right]. \tag{16}$$

In a similar way, we can know the force condition of lateral disturbing force shown in Figure 7(b) is

$$\begin{cases} \sum \boldsymbol{\mathcal{L}} = (\boldsymbol{\mathcal{F}}_f \times \boldsymbol{\mathcal{A}}\boldsymbol{\mathcal{O}}) + (\boldsymbol{\mathcal{F}}'_f \times \boldsymbol{\mathcal{A}}'\boldsymbol{\mathcal{O}}) = \boldsymbol{0}, \\ F_P = 2PS, \\ F_{fi\max} = \mu(F_N + 2PS), \\ F_{f\,\max_{xz}} = F_{f\max}\cos\frac{\alpha}{2}, \\ F_{N_z} = F_N\sin\frac{\alpha}{2}, \\ F_{P_z} = F_P\sin\frac{\alpha}{2}, \\ F_2^2 + (2F_{N_z} - 2F_{P_z})^2 \le (2F_{f\,\max_{xz}})^2. \end{cases} \tag{17}$$

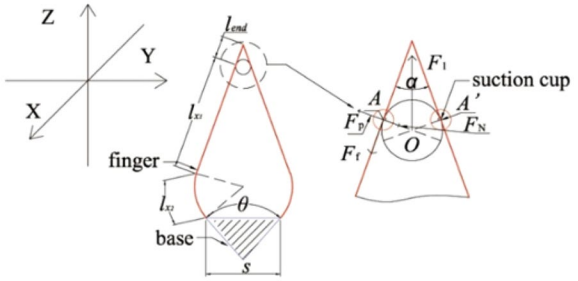


**a** Schematic diagram of tension

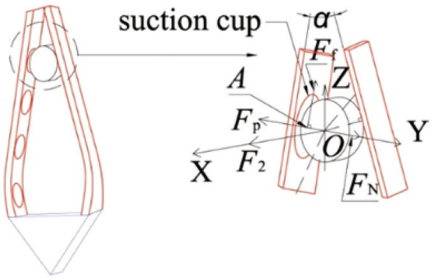


**b** Schematic diagram of lateral disturbing force

**Figure 7** Grasping schematic diagram of SOHE

Combining Eqs. (14) and (17), then simplifying result in

$$F_{2\max} = 2\left\{\left[\mu(F_N + 2PS)\cos\left(\arctan\left(\frac{r}{l_{x1}+l_{end}}\right)\right)\right]^2 - \left[(F_N - 2PS)\sin\left(\arctan\left(\frac{r}{l_{x1}+l_{end}}\right)\right)\right]^2\right\}^{\frac{1}{2}}. \tag{18}$$

## 4 Experiment of the STU Hand with Half-Enveloping Grasping Mode

To evaluate performances of the STU hand with half-enveloping grasping mode, this part conducts several experiments on load capacity and stability with permissible size and the versatility of the STU hand. The load capacity is equivalent to the tension in the vertical direction minus gravity of object likes $F_1$. The stability is evaluated by the lateral disturbing force likes $F_2$. $F_1$ and $F_2$ are shown in both Figure 6 and Figure 7. The intrinsic parameters of the STU used in the following experiments are listed in Table 2. Substituting these parameters into Eqs. (2), (3) and (5), we have $R_{\max}^{BOHE} = 177$ mm, $R_{\min}^{BOHE} = 74$ mm, $R^{SHOE} = 4$ mm. The cylinders used for evaluating the load capacity and stability are made of double sided sponge tape. As a result of attaching different materials to surface of tape, we can change the friction coefficient. Contraposing the three grasping types mentioned in Section 3, we respectively test some materials which is common in daily life to capture data, four materials a type, ten tests a material. The four materials are A4 paper, polyethylene plastics, silica gel and tinfoil. We use the NK-30 push-pull dynamometer produced by HANDPI Company to measure force. The accuracy of this production is 0.1 N.

**Table 2 Value of intrinsic parameters**

| Parameter | Value |
|---|---|
| $s$ (mm) | 35 |
| $\theta$ (rad) | 2.093 |
| $l$ (mm) | 100 |
| $l_{end}$ (mm) | 18 |

### 4.1 Evaluate Grasping Ability of BOHE

When the size of object is $R_{\max}^{BOHE}$, the $F_1$ is greater than $F_2$ for all materials as shown in Figure 8. Because the grasping force mainly projects on the direction of $F_1$. This causes the object away from the gripper more easily. If the material is polyethylene plastics, the tension and lateral disturbing force reach maximal value at 16.24 N and 21.94 N, respectively. When the radius of object gradually decreases to $R_{\min}^{BOHE}$, the grasping force is more helpful to hold the object. So, the $F_2$ is greater than $F_1$ in this situation shown in Figure 9. The tension and lateral disturbing force also reach the maximal value while the material is polyethylene plastics. They are 34.0 N and 33.0 N, respectively. For BOHE grasping mode, obviously, the smaller object size is, the better performances of the STU hand on load capacity and stability are.

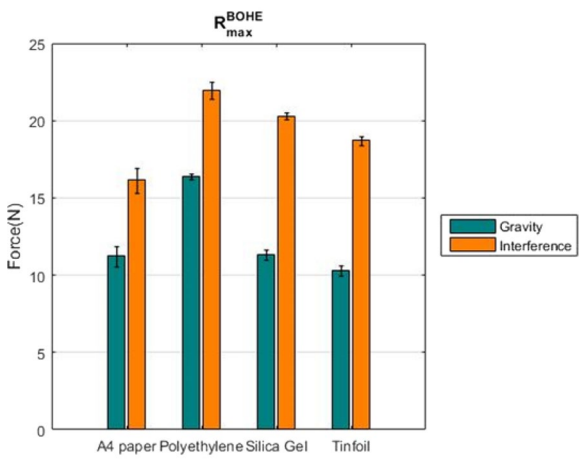


**Figure 8** Grasping ability of BOHE grasping mode with the maximal object size

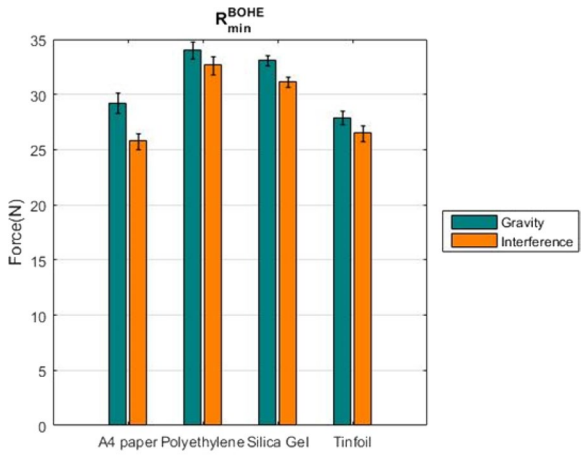


**Figure 9** Grasping ability of BOHE grasping mode with the minimal object size

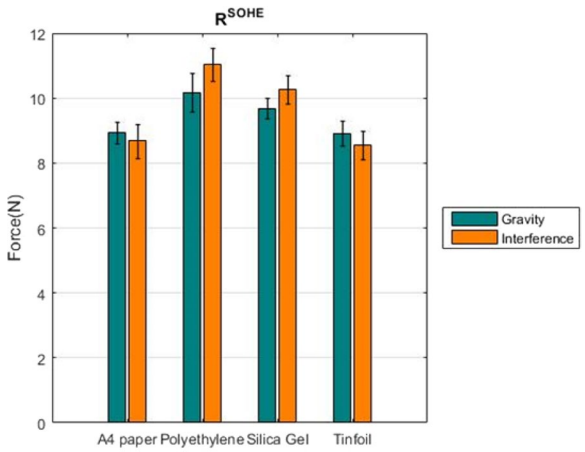


**Figure 10** Grasping ability of SOHE grasping mode

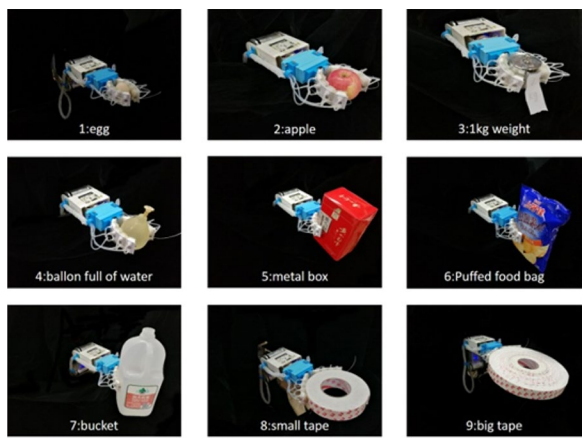


**Figure 11** Grasp various objects using the STU hand (Additional file 1)

### 4.2 Evaluate Grasping Ability of SOHE

Here comes the far more smaller object with the radius of $R^{SOHE}$ and the STU hand works in the SOHE grasping mode in the meantime. In this situation, the positive pressure exerted on object is almost 0 because the fingertips touch each other. And the $\alpha$ in Eq. (14) can be determined as 0.134 rad. According to the two constraints, Eqs. (16) and (18) can be simplified as $F_1 \approx 4PS$ and $F_1 \approx 4PS\sqrt{\mu}$. Consequently, the material influences the value relationship between $F_1$ and $F_2$. And the tension and lateral disturbing force should be almost equal because $\sqrt{\mu}$ approximates 1. The conclusion can match with the diagram shown in Figure 10.

### 4.3 Object Grasping

Except for the half-enveloping grasping, there are three more grasping modes for the STU hand. As shown in Figure 11, the STU hand can grasp objects covering a large range of sizes and divers shapes by choosing suitable grasping mode. The 8th object has the minimal size of BOHE grasping mode and the 9th object has the maximal size of BOHE.

## 5 Conclusions

(1) This paper proposes a half-enveloping grasping mode aiming to acquiring a wide range of object sizes, even when the force closure is failure. Notable features used to meet these goals are the suction cups which provide the suction force to prohibit object to be extruded.

(2) To determine the effective range of object sizes the STU hand can grasp and the grasping force with half-enveloping grasping mode definitely we did a lot of calculation and analysis. What surprises us is that the grasping size ratio between the biggest object and the smallest one is beyond 40 for the STU hand used in experiment.

(3) After evaluating the load capacity and stability with half-enveloping grasping mode in experiment, we find that even when the STU hand grasps the small object (8 mm diameter), the minimal tension and lateral disturbing force are over 8 N.

## Additional file

**Additional file 1.** Video of grasping various objects.

**Authors' contributions**

Pei-Chen Wu was in charge of the whole trial and wrote the manuscript except for Section 3 and Section 4. Nan Lin was in charge of Section 3 and Section 4. Ting Lei wrote the Section 3 and Jin-Ze Wu wrote the Section 4. Qian Cheng assisted with sampling and laboratory analyses. Xiao-Ping Chen offered guidance. All authors read and approved the final manuscript.

**Authors' Information**

Pei-Chen Wu, born in 1994, is currently a master candidate at *University of Science and Technology of China*. He received his bachelor degree from *Zhengzhou University, China*, in 2016. His research interests include soft robotics design and motion planning.

Nan Lin, born in 1993, is currently a master candidate at *University of Science and Technology of China*. He received his bachelor degree from *University of Science and Technology of China*, in 2016. His research interests include soft robotics design and motion planning.

Ting Lei, born in 1998, is currently an undergraduate at *School of Computer Science and Technology, University of Science and Technology of China*.

Qian Cheng, born in 1996, is currently an undergraduate at *School of Information Science and Technology, University of Science and Technology of China*.

Jin-Ze Wu, born in 1997, is currently an undergraduate at *School of Computer Science and Technology, University of Science and Technology of China*.

Xiao-Ping Chen, born in 1955, is currently a professor at *Computer Science at University of Science and Technology of China*. His current research interests include AI logic agent learning, multi-robot systems and soft robotics.

**Competing interests**

The authors declare that they have no competing interests.

**Funding**

Supported by National Natural Science Foundation of China (Grant Nos. U1613216, 61573333).

## Publisher's Note



Received: 23 November 2017 Accepted: 8 October 2018
Published online: 14 November 2018

**References**

[1] Deimel, O Brock. A novel type of compliant and underactuated robotic hand for dexterous grasping. *The International Journal of Robotics Research*, 2016, 35(1-3): 161-185.
[2] D M Aukes, B Heyneman, J Ulmen, et al. Design and testing of a selectively compliant underactuated hand. *The International Journal of Robotics Research*, 2014, 33(5): 721-735.
[3] S C Jacobsen, J E Wood, D F Knutti, et al. The UTAH/MIT dextrous hand: Work in progress. *The International Journal of Robotics Research*, 1984, 3(4): 21-50.
[4] C Cipriani, M Controzzi, M C Carrozza. The SmartHand transradial prosthesis. *Journal of Neuroengineering and Rehabilitation*, 2011, 8(1): 29.
[5] H Kawasaki, T Komatsu, K Uchiyama. Dexterous anthropomorphic robot hand with distributed tactile sensor: Gifu hand II. *IEEE/ASME Transactions on Mechatronics*, 2002, 7(3): 296-303.
[6] H Liu, P Meusel, N Seitz, et al. The modular multisensory DLR-HIT-Hand. *Mechanism and Machine Theory*, 2007, 42(5): 612-625.
[7] M Grebenstein, M Chalon, W Friedl, et al. The hand of the DLR and arm system: Designed for interaction. *The International Journal of Robotics Research*, 2012, 31(13): 1531-1555.
[8] K B Shimoga. Robot grasp synthesis algorithms: A survey. *The International Journal of Robotics Research*, 1996, 15(3): 230-266.
[9] A Saxena, J Driemeyer, A Y Ng. Robotic grasping of novel objects using vision. *The International Journal of Robotics Research*, 2008, 27(2): 157-173.
[10] B Jin, L X Lin. Design and force control of an underactuated robotic hand for fruit and vegetable picking. *Journal of Mechanical Engineering*, 2014, 50(19): 1-8. (in Chinese)
[11] L C Wu, Y X Kong, X L Li. Fully rotational joint underactuated finger mechanism and its kinematics analysis. *Journal of Mechanical Engineering*, 2017, 53(1): 47-54. (in Chinese)
[12] B Belzile, L Birglen. A compliant self-adaptive gripper with proprioceptive haptic feedback. *Autonomous Robots*, 2014, 36(1-2): 79-91.
[13] B Gao, L Lei, S Zhao, et al. A novel underactuated hand with adaptive robotic fingers. *Proceedings of the IEEE International Conference on Information and Automation*, Zhejiang, China, July 31–August 4, 2016:1392–1397.
[14] Y Yang, X Xu, W Zhang. A parallel and self-adaptive underactuated finger with novel belt and cam-link mechanisms. *Proceedings of the IEEE International Conference on Advanced Robotics and Mechatronics*, Macau, China, August 18–20, 2016:635–639.
[15] F Ilievski, A D Mazzeo, R F Shepherd, et al. Soft robotics for chemists. *Angewandte Chemie*, 2011, 123(8): 1930-1935.
[16] A A Stokes, R F Shepherd, S A Morin, et al. A hybrid combining hard and soft robots. *Soft Robotics*, 2014;1(1):70–74.
[17] R Deimel, O Brock. A compliant hand based on a novel pneumatic actuator. *Proceedings of the IEEE International Conference on Robotics and Automation*, Karlsruhe, Germany, May 6–10 2013:2047–2053.
[18] B S Homberg, R K Katzschmann, M R Dogar, et al. Haptic identification of objects using a modular soft robotic gripper. *Proceedings of IEEE/RSJ Conference on Intelligent Robots and Systems,* Hamburg, Germany, September 28–October 3, 2015:1698–1705.
[19] T M Wang, T Wang, J Hong, et al. Soft Robotics: Structure, Actuation, Sensing and Control. *Journal of Mechanical Engineering,* 2017, 53(13): 1-13. (in Chinese)
[20] E Brown, N Rodenberg, J Amend, et al. Universal robotic gripper based on the jamming of granular material. *Proceedings of the National Academy of Sciences*, 2010;107(44):18809–18814.
[21] J R Amend, E Brown, N Rodenberg, et al. A positive pressure universal gripper based on the jamming of granular material. *IEEE Transactions on Robotics*, 2012;28(2):341–350.
[22] B Mishra, N Silver. Some discussion of static gripping and its stability. *IEEE Transactions on Systems, Man, and Cybernetics*, 1989;19(4):783–796.
[23] M Cutkosky, P Wright. Modeling manufacturing grips and correlations with the design of robotic hands. *Proceedings of IEEE International Conference on Robotics and Automation*, San Francisco, USA, April, 1986;3:1533–1539.
[24] D Lyons. A simple set of grasps for a dextrous hand. *Proceedings of IEEE International Conference on Robotics and Automation*, Missouri, USA, March 25–28, 1985;2:588–593.
[25] T Iberall. The nature of human prehension: Three dextrous hands in one. *Proceedings of IEEE International Conference on Robotics and Automation*, Carolina, USA, March 31–April 3, 1987;4:396–401.
[26] J R Napier. The prehensile movements of the human hand. *Bone & Joint Journal*, 1956, 38(4): 902-913.
[27] J Ponce, B Faverjon. On computing three-finger force-closure grasps of polygonal objects. *IEEE Transactions on Robotics and Automation*, 1995, 11(6): 868-881.
[28] B Dizioğlu, K Lakshiminarayana. Mechanics of form closure. *Acta Mechanica*, 1984, 52(1): 107-118.
[29] V D Nguyen. Constructing force-closure grasps. *The International Journal of Robotics Research*, 1988, 7(3): 3-16.